

Magnetoacoustic Resonance to Probe Quadrupole–Strain Coupling in a Diamond Nitrogen-Vacancy Center as a Spin-Triplet System

Mikito Koga¹ and Masashige Matsumoto²

¹*Department of Physics, Faculty of Education, Shizuoka University, Shizuoka 422–8529, Japan*

²*Department of Physics, Faculty of Science, Shizuoka University, Shizuoka 422–8529, Japan*

A theory of magnetoacoustic resonance is proposed to measure quadrupole–strain couplings in a spin-triplet state with the C_{3v} point group symmetry, considering the spin–strain interaction in a diamond nitrogen-vacancy (NV) center. Based on the Floquet theory, we demonstrate how the single- and two-phonon transition probabilities depend on the change in the longitudinal and transverse quadrupole couplings, which can be controlled by rotating an applied magnetic field, around the threefold axis. The obtained quadrupole dynamics results are useful for realizing mechanical or ac strain-control of the NV spin as an alternative to the conventional magnetic control by spin resonance.

The negatively charged nitrogen-vacancy (NV) center in diamond is a unique defect in which the spin degrees of freedom are described by spin-1 ($S = 1$) in a C_{3v} crystalline-electric-field environment.^{1–4} A long coherence time of over a millisecond is a significant advantage for the robustness of the spin state at room temperature.^{5–7} Thus, the NV center is a good candidate for a promising platform for spin-controlled devices for quantum information processing and sensing applications.⁸ Since the $S = 1$ spin operator $\mathbf{S} = (S_x, S_y, S_z)$ contains quadrupole degrees of freedom, the electronic spin is coupled to local strains owing to the crystal lattice deformations. There are five components of quadrupole operators: $O_u = (2S_z^2 - S_x^2 - S_y^2)/\sqrt{3}$, $O_v = S_x^2 - S_y^2$, $O_{xy} = S_x S_y + S_y S_x$, $O_{zx} = S_z S_x + S_x S_z$, and $O_{yz} = S_y S_z + S_z S_y$.

Recently, a theoretical proposal for mechanically and electrically driven electron spin resonance has shed light on the important role of spin–strain interaction in the spin-triplet ground state of the NV defect,⁹ which is split into lower singlet ($S_z = 0$) and higher doublet ($S_z = \pm 1$) energy levels by a uniaxial crystal field along the threefold axis. This work has pointed out the relevance of O_{zx} and O_{yz} to electrical or mechanical control of the NV spin, although not much attention has been paid to these quadrupoles to date.^{10–14} Since only O_u , O_v , and O_{xy} have been considered for such spin control,^{15–17} the confirmation of O_{zx} and O_{yz} is highly desired for pursuit of various methods of electrical or mechanical spin control as an alternative to conventional magnetic control.^{18,19} Note that O_u , O_v , and O_{xy} cause the transition in the doublet, whereas O_{zx} and O_{yz} are involved in the transition between the singlet and doublet levels. Very recently, an evaluation of spin–strain coupling with O_{zx} has been performed by measurements of an acoustically driven single-quantum spin transition.²⁰ As reported in our recent studies,^{21,22} it is also important that the transition via quadrupole couplings can be changed by rotating an applied magnetic field. This is useful for probing such a spin–strain coupling with O_{zx} that is difficult to measure.

In this study, we present a new idea of magnetoacoustic resonance for ultrasonic measurements of spin–strain coupling parameters in the $S = 1$ spin state, considering the NV spin as a typical example. This was first motivated by the discovery of an extremely strong strain coupling inherent in

boron-doped silicon vacancies by elastic softening measurements.^{23,24} In the NV center, phonon-assisted orbital transitions driven by an acoustic wave were detected by photoluminescence excitation spectroscopy²⁵ as well as an acoustically driven transition in the spin-triplet state.²⁰ Thus, the vacancy states with quadrupoles commonly possess high sensitivity to local strains or lattice vibrations.

We study a simplified spin–strain interaction in the electronic $S = 1$ spin state, considering that the lattice deformations are limited in the plane including the [001] and [110] crystal axes. Using the above quadrupole operators in the C_{3v} frame (NV axis frame), the spin–strain interaction Hamiltonian can be written as^{9,26}

$$H_\varepsilon = \sum_k A_{k,\varepsilon} O_k \quad (k = u, v, zx), \quad (1)$$

where $A_{k,\varepsilon}$ is a strain-dependent coupling coefficient with each quadrupole, and both $A_{xy,\varepsilon}$ and $A_{yz,\varepsilon}$ vanish owing to the limited lattice deformations. The z -axis is chosen in the direction of a threefold axis vector $\mathbf{e}_z = (1, 1, 1)/\sqrt{3}$, and the two other orthogonal basis vectors are defined as $\mathbf{e}_y = (1, -1, 0)/\sqrt{2}$ and $\mathbf{e}_x = (-1, -1, 2)/\sqrt{6}$. The coupling coefficients are given by $A_{u,\varepsilon} = g_u \varepsilon_1$, $A_{v,\varepsilon} = (g_b \varepsilon_{U_1} + g_c \varepsilon_{U_2})/\sqrt{3}$, and $A_{zx,\varepsilon} = (2g_d \varepsilon_{U_1} - g_e \varepsilon_{U_2})/\sqrt{6}$, where $\varepsilon_1 = (\varepsilon_{YZ} + \varepsilon_{ZX} + \varepsilon_{XY})/\sqrt{3}$, $\varepsilon_{U_1} = (2\varepsilon_{ZZ} - \varepsilon_{XX} - \varepsilon_{YY})/\sqrt{3}$, and $\varepsilon_{U_2} = (2\varepsilon_{XY} - \varepsilon_{YZ} - \varepsilon_{ZX})/\sqrt{3}$. The strain tensors are denoted by $\varepsilon_{ij} = [(\partial u_i / \partial x_j) + (\partial u_j / \partial x_i)]/2$ with the displacement vector $\mathbf{u} = (u_1, u_2, u_3) = (u_X, u_Y, u_Z)$, and $(x_1, x_2, x_3) = (X, Y, Z)$ is the cubic crystal coordinate. There are five independent coupling parameters g_i ($i = a, b, c, d, e$), and bulk strain $\varepsilon_{XX} + \varepsilon_{YY} + \varepsilon_{ZZ}$ has been disregarded.

In the C_{3v} (xyz) frame, the electronic $S = 1$ states are described by the following local Hamiltonian:

$$H_l = -h(S_x \cos \phi + S_y \sin \phi) + \sqrt{3} D O_u, \quad (2)$$

where $h = \gamma_e H$ for the magnetic field $\mathbf{H} = (H \cos \phi, H \sin \phi, 0)$ ($\gamma_e = 2.8$ MHz/G is the electron gyromagnetic ratio). In the last term, $3D$ (> 0) equals the energy of the doublet excited state measured from the singlet ground state for $H = 0$ and this splitting is 2.87 GHz for the NV center. The doublet state is split by the magnetic field, and we neglect the higher-lying state assuming that h

is sufficiently large compared to $A_{k,\varepsilon}$ in Eq. (1). Note that the energies of the three spin states do not depend on the field direction ϕ perpendicular to the threefold axis. After diagonalizing H_1 , the eigenvalue and eigenfunction of the ground state are obtained as

$$\frac{E_1}{D} = \frac{1}{2}(-1 - \alpha) \left(\alpha = \sqrt{9 + 4\bar{h}^2}, \bar{h} = \frac{h}{D} \right), \quad (3)$$

$$|\psi_1\rangle = \frac{\sin\chi}{\sqrt{2}}e^{-i\phi}|+1\rangle + \cos\chi|0\rangle + \frac{\sin\chi}{\sqrt{2}}e^{i\phi}|-1\rangle, \quad (4)$$

respectively, based on the eigenstates $|m\rangle$ ($m = 0, \pm 1$) of S_z . For the first excited state, we obtain

$$\frac{E_2}{D} = 1, \quad |\psi_2\rangle = \frac{1}{\sqrt{2}}e^{-i\phi}|+1\rangle - \frac{1}{\sqrt{2}}e^{i\phi}|-1\rangle. \quad (5)$$

The coefficients in Eq. (4) are given by

$$\cos\chi = \sqrt{\frac{1}{2}\left(1 + \frac{3}{2\bar{\varepsilon}_0 - 3}\right)}, \quad \sin\chi = \sqrt{\frac{1}{2}\left(1 - \frac{3}{2\bar{\varepsilon}_0 - 3}\right)}, \quad (6)$$

where $\bar{\varepsilon}_0 = (E_2 - E_1)/D = (3 + \alpha)/2$. Since $\bar{\varepsilon}_0 > 3$ must be satisfied, χ varies in $0 < \chi < \pi/4$.

Next, we derive an effective spin-strain interaction Hamiltonian in the subspace of the above two states $|\psi_\mu\rangle$ ($\mu = 1, 2$) coupled to time-dependent oscillating strain fields ε_λ ($\lambda = 1, U_1, U_2$), which are driven by an acoustic wave propagating in the lattice. The time dependency is represented by $\varepsilon_\lambda = a_\lambda \cos \omega t$, where ω is the acoustic-wave frequency and a_λ is the vibration amplitude. The relative phase shifts between the three components are not considered for simplicity. By calculating $\langle \psi_\mu | H_\varepsilon | \psi_\nu \rangle$ ($\mu, \nu = 1, 2$), we obtain the following form of the effective Hamiltonian for the two-level system coupled to the periodically time-dependent strains,

$$H_{\text{eff}}(t) = \frac{1}{2} \begin{pmatrix} -\varepsilon_0 - A_L \cos \omega t & A_T \cos \omega t \\ A_T^* \cos \omega t & \varepsilon_0 + A_L \cos \omega t \end{pmatrix}. \quad (7)$$

Here, $\varepsilon_0 = \bar{\varepsilon}_0 D$ is the level splitting of the two states. The longitudinal ($A_L \cos \omega t = \langle \psi_2 | H_\varepsilon | \psi_2 \rangle - \langle \psi_1 | H_\varepsilon | \psi_1 \rangle$) and transverse ($A_T \cos \omega t = 2\langle \psi_1 | H_\varepsilon | \psi_2 \rangle$) couplings depend on the magnetic field direction ϕ and the $\bar{\varepsilon}_0$ -dependent trigonometric functions in Eq. (6),

$$A_L = \frac{\sqrt{3}}{2}(1 + \cos 2\chi)A_u - \frac{1}{2}(3 - \cos 2\chi)\cos 2\phi \cdot A_v, \quad (8)$$

$$A_T = 2(-i \sin \chi \sin 2\phi \cdot A_v + \cos \chi \cos \phi \cdot A_{zx}). \quad (9)$$

For the quadrupole-strain couplings, $A_u = g_a a_1$, $A_v = (g_b a_{U_1} + g_c a_{U_2})/\sqrt{3}$, and $A_{zx} = (2g_d a_{U_1} - g_e a_{U_2})/\sqrt{6}$.

Similar forms of the time-dependent Hamiltonian in Eq. (7) has been frequently studied by the Floquet theory.^{21, 22, 27-30} Following Shirley,²⁷ the problem of solving the time-dependent Schrödinger equation is transformed to a time-independent eigenvalue problem using an infinite-dimensional matrix form of the Floquet Hamiltonian. The matrix element $\langle \alpha n | H_F | \beta m \rangle = H_{\alpha\beta}^{[n-m]} + n\omega\delta_{nm}\delta_{\alpha\beta}$ is constructed using the Floquet states $|\alpha n\rangle = |\alpha\rangle \otimes |n\rangle$. Here, α ($= \psi_1, \psi_2$) and n ($= 0, \pm 1, \pm 2, \dots$) denote one of the two levels and the time dependency $e^{in\omega t}$, respectively, and $\hbar = 1$ is used. The block matrix $H^{[n-m]}$ is only finite for $n - m = 0, \pm 1$. In the

Floquet matrix represented by

$$H_F = \begin{pmatrix} \ddots & & & & & \\ & H_{-2}^{[0]} & H^{[-1]} & \mathbf{0} & \mathbf{0} & \mathbf{0} \\ & H_{-1}^{[1]} & H_{-1}^{[0]} & H^{[-1]} & \mathbf{0} & \mathbf{0} \\ \cdots & \mathbf{0} & H_{-1}^{[1]} & H_0^{[0]} & H^{[-1]} & \mathbf{0} \\ & \mathbf{0} & \mathbf{0} & H_{-1}^{[1]} & H_1^{[0]} & H^{[-1]} \\ & \mathbf{0} & \mathbf{0} & \mathbf{0} & H_{-1}^{[1]} & H_2^{[0]} \\ & & & & & \ddots \end{pmatrix}, \quad (10)$$

the diagonal sectors are defined as

$$H_n^{[0]} \equiv H^{[0]} + n\omega = \begin{pmatrix} -(\varepsilon_0/2) + n\omega & 0 \\ 0 & (\varepsilon_0/2) + n\omega \end{pmatrix}, \quad (11)$$

and the off-diagonal sectors are given by

$$H^{[\pm 1]} = \frac{1}{4} \begin{pmatrix} -A_L & A_T \\ A_T^* & A_L \end{pmatrix}. \quad (12)$$

In Eq. (10), $\mathbf{0}$ represents the 2×2 form of the zero matrix. The eigenvalue problem is described by, $H_F |q_\gamma\rangle = q_\gamma |q_\gamma\rangle$, where the γ th eigenvalue q_γ is termed the quasienergy and $|q_\gamma\rangle$ is the corresponding eigenfunction. For the time-averaged transition probability between the α and β states, we use the following formula: $\bar{P}_{\alpha \rightarrow \beta} = \sum_m \sum_\gamma |\langle \beta m | q_\gamma \rangle \langle q_\gamma | \alpha 0 \rangle|^2$.^{27, 29}

In particular, we focus on the emergence of transition probability peaks expected for the nearly degenerate Floquet states, for instance, $|\alpha 0\rangle$ and $|\beta, -n\rangle$, where $-\varepsilon_0/2 \approx \varepsilon_0/2 - n\omega$ is satisfied. In this case, the infinite-dimensional matrix form of H_F is reduced to an effective 2×2 matrix using the Van Vleck perturbation theory.^{29, 30} By analogy with previous studies,^{21, 22} the effective Hamiltonian in the subspace of $|\alpha 0\rangle$ and $|\beta, -n\rangle$ is given by

$$\tilde{H}_F = \begin{pmatrix} -(\varepsilon_0/2) + \delta_n & v_{-n} \\ v_{-n}^* & (\varepsilon_0/2) - \delta_n - n\omega \end{pmatrix}. \quad (13)$$

Here, the off-diagonal matrix element $v_{-n} = (-n\omega/2)J_{-n}(A_L/\omega)A_T/A_L$ is calculated up to the first order of A_T using the k th Bessel function of the first kind J_k . The leading term of the energy shift δ_n is given as $\delta_n = -\sum_{k \neq -n} |v_k|^2 / (\varepsilon_0 + k\omega)$. The diagonalization of \tilde{H}_F gives the eigenvalues $q_\pm = -(\varepsilon_0/2) \pm \tilde{q}_n$, where $\tilde{q}_n = \sqrt{(n\omega - \varepsilon_0 + 2\delta_n)^2/4 + |v_{-n}|^2}$, and leads to the time-averaged transition probability represented by $\bar{P}_{\psi_1 \rightarrow \psi_2}^{(n)} = (1/2)|v_{-n}|^2/\tilde{q}_n^2$. This is valid for $n = 1$ and $n = 2$, which correspond to the single- and two-phonon transition processes, respectively, because the higher-order terms with A_T must be considered for $n \geq 3$. In the weak coupling limit ($|A_L|/\omega, |A_T|/\omega \ll 1$), $|v_{-n}| \approx \{|A_T|/[2^{n+1}(n-1)!]\}(|A_L|/\omega)^{n-1}$ ($n \geq 1$) leads to simple analytic forms for the transition probability at fixed $\varepsilon_0 = n\omega$ ($n = 1, 2$) as²²

$$\bar{P}_{\psi_1 \rightarrow \psi_2}^{(1)}(\varepsilon_0 = \omega) = \frac{1}{2} \frac{1}{1 + [|A_T|/(8\omega)]^2}, \quad (14)$$

$$\bar{P}_{\psi_1 \rightarrow \psi_2}^{(2)}(\varepsilon_0 = 2\omega) = \frac{1}{2} \frac{1}{1 + (4/9)(|A_T|/|A_L|)^2}, \quad (15)$$

for finite $|A_T|$, and $\bar{P}_{\psi_1 \rightarrow \psi_2}^{(n)}$ vanishes for $A_T = 0$.

In Eq. (15), the two-phonon transition probability strongly depends on $|A_T|^2/|A_L|^2$, and it vanishes, especially when A_L

approaches zero. It must be noted that the longitudinal (A_L) coupling is required for the two-phonon transition process as well as the transverse (A_T) coupling, as pointed out in $S = 1/2$ spin systems.³¹⁾ This is completely unlike the single-phonon transition process dominated by A_T . Since the quadrupole-strain couplings A_L and A_T depend on the rotation angle ϕ of the magnetic field, $P^{(2)}$ in Eq. (15) changes with ϕ . From Eqs. (8) and (9), the ϕ dependence is given by

$$\frac{|A_T|^2}{|A_L|^2} = \frac{16}{9} \frac{A_{zx}^2 \cos^2 \chi \cos^2 \phi + A_v^2 \sin^2 \chi \sin^2 2\phi}{\left[\frac{A_u}{\sqrt{3}} (1 + \cos 2\chi) - A_v \left(1 - \frac{\cos 2\chi}{3} \right) \cos 2\phi \right]^2}. \quad (16)$$

Here, χ is given by substituting $\bar{\epsilon}_0 = 2\omega/D$ in Eq. (6) and is independent of ϕ . The ratios between the three couplings A_u , A_v , and A_{zx} can be evaluated by $\bar{P}^{(2)}$ as a function of ϕ in Eqs. (15) and (16). There exist characteristic field directions ϕ_0 at which $\bar{P}^{(2)} \rightarrow 0$, namely, $A_L \rightarrow 0$. The ratio A_u/A_v is obtained from

$$\cos 2\phi_0 = \frac{A_u}{\sqrt{3}A_v} \frac{1 + \cos 2\chi}{1 - (\cos 2\chi)/3}, \quad (17)$$

and the absolute value of the right-hand side must be less than unity. This evaluation is also valid for a stronger coupling case ($|A_T|/\omega, |A_L|/\omega \simeq 1$), as discussed later, and $\bar{P}^{(2)}$ shows a minimum at $\phi \simeq \phi_0$. For $|A_u/A_v| > \sqrt{3}$, no minimum is found in $0 < \phi < \pi$. In addition, for the weak coupling, the ratio A_{zx}/A_v is related to the value of $\bar{P}^{(2)}$ at $\phi = 0$ as

$$\bar{P}^{(2)}(\phi = 0) = \frac{1}{2} \left\{ 1 + \left[\frac{8}{9} C(\chi, \phi_0) \frac{A_{zx}}{A_v} \right]^2 \right\}^{-1}, \quad (18)$$

where $C(\chi, \phi_0) = \cos \chi / \{ [1 - (\cos 2\chi)/3] (1 - \cos 2\phi_0) \}$. Thus, the ratios between the quadrupole couplings can be probed by the field angle dependence of $\bar{P}^{(2)}(\phi)$ at $\epsilon_0 = 2\omega$. In particular, for $A_v \gg A_u, A_{zx}$, $\bar{P}^{(2)}(\phi)$ shows fourfold symmetry in rotating the magnetic field around the z axis, namely, $[111]$, and it continuously approaches zero at $\phi = \pi/4$ in $0 < \phi < \pi/2$. As given by Eq. (17), ϕ for $\bar{P}^{(2)} \rightarrow 0$ shifts to a lower value from $\pi/4$ with an increase in A_u . In addition, the value of $\bar{P}^{(2)}(\phi = 0)$ decreases from $1/2$ as A_{zx}/A_v increases. Such features become more prominent in the weak coupling case.

First, let us consider the $A_u = 0$ case where the longitudinal coupling A_L depends only on A_v . Figures 1 (a) and (b) show the contour maps of the transition probability \bar{P} calculated numerically using the Floquet matrix, which are plotted as a function of ϕ and ϵ_0/ω [$\epsilon_0 = (3D + \sqrt{9D^2 + 4h^2})/2$]. In both cases, \bar{P} completely vanishes at $\phi/\pi = 1/2$ for all values of ϵ_0 owing to $A_T = 0$ [see Eq. (9)]. This indicates that the field direction $\phi/\pi = 1/2$ is very specific to the quadrupole-strain coupling, which is parallel to $\mathbf{e}_y \parallel [1\bar{1}0]$ and perpendicular to the threefold axis. The most prominent feature is the existence of a resonance peak at around $\epsilon_0/\omega = 1$ associated with the single-phonon transition probability $\bar{P}^{(1)}$. In the weak coupling limit, the peak broadening $2|v_{-1}|$ is proportional to $|A_T|$. The ϕ dependence of $|A_T|$ explains the maximum broadening at $\phi/\pi \simeq 1/4$ for $A_v > A_{zx}$ in Fig. 1 (a), which reflects $\sin 2\phi$ for coupling with the $x^2 - y^2$ quadrupole in Eq. (9).²²⁾ Conversely, the maximum broadening shifts toward $\phi = 0$ as A_{zx}/A_v increases in Fig. 1 (b), owing to $\cos \phi$ for the coupling with the zx quadrupole.

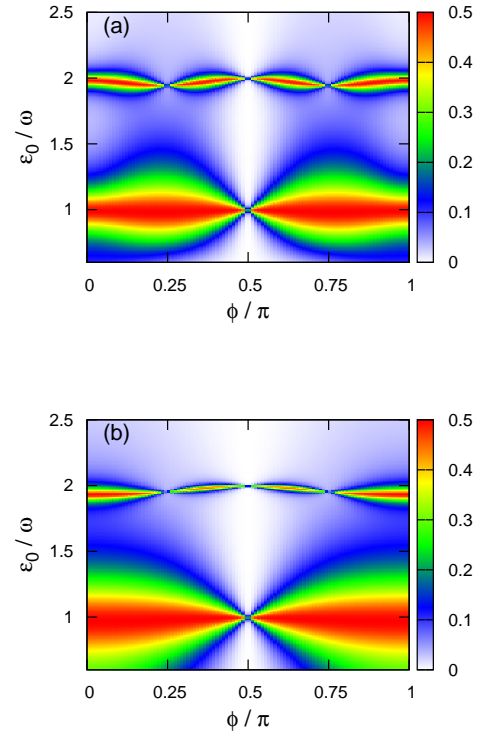


Fig. 1. (Color online) Contour map of the transition probability as a function of ϕ and ϵ_0/ω . (a) $A_u = 0$, $A_v/\omega = 0.4$, and $A_{zx}/\omega = 0.2$. (b) $A_u = 0$, $A_v/\omega = 0.2$, and $A_{zx}/\omega = 0.4$. Here, $\epsilon_0/\omega > 0.6$ because D/ω is fixed at 0.2.

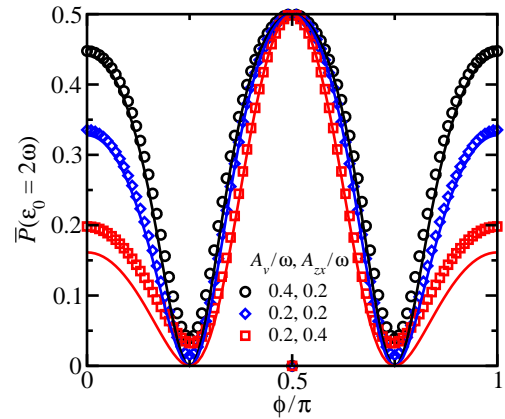


Fig. 2. (Color online) Transition probability at $\epsilon_0 = 2\omega$ as a function of ϕ , where each data point is plotted for $D/\omega = 0.2$ and $A_u = 0$. The black circles, blue diamonds, and red squares represent the data for $(A_v, A_{zx}) = (0.4, 0.2)$, $(0.2, 0.2)$, and $(0.2, 0.4)$ in units of ω , respectively. The solid lines are drawn for $A_{zx}/A_v = 1/2$ (black), 1 (blue), and 2 (red) in the weak coupling limit.

To evaluate the spin-strain coupling parameters g_i , we focus on the two-phonon transition process at around $\epsilon_0 = 2\omega$, although $\bar{P}^{(2)}$ shows a much narrower resonance peak in the weak coupling limit. The two-phonon transition is dominated by longitudinal coupling with A_L . $\bar{P}(\epsilon_0/\omega = 2)$ approaches the maximum $1/2$ for $|A_L| \gg |A_T| > 0$, whereas it is strongly dependent on $|A_L|$, even when $|A_T| \simeq |A_L|$.

Figure 2 shows $\bar{P}(\epsilon_0/\omega = 2)$ as a function of ϕ for various values of A_v and A_{zx} , where A_u is fixed at zero. The ratio

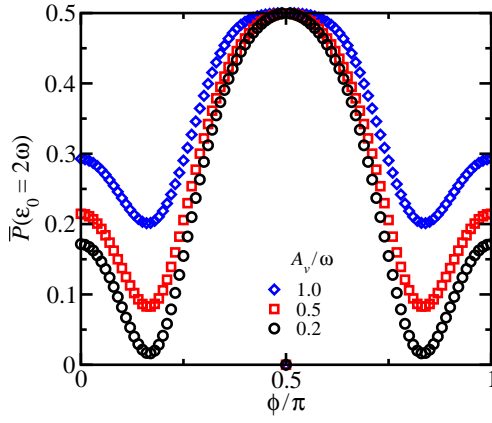


Fig. 3. (Color online) Transition probability at $\varepsilon_0 = 2\omega$ as a function of ϕ for various values of A_v/ω , where $D/\omega = 0.2$ and $A_u/(\sqrt{3}A_v) = 0.4$, and $A_{zx}/A_v = 1$ are fixed. The results for $A_v/\omega = 0.2, 0.5$, and 1.0 are plotted as circles, squares, and diamonds, respectively.

A_{zx}/A_v is determined from the value at $\phi/\pi = 0$ or 1 as a local maximum. This value decreases with the increase in A_{zx}/A_v as expected from Eq. (18). For $A_{zx}/A_v > 1$ in Fig. 2 (red squares), the relatively large deviations from the weak coupling limit at around $\phi/\pi = 0$ and 1 is owing to the larger contribution from higher order terms with A_{zx} compared to those with A_v . For $A_u = 0$, the spin-strain coupling parameters g_i can be evaluated by choosing a quadrupole coupling with a single-strain component ε_{U_1} ($\varepsilon_1 = \varepsilon_{U_2} = 0$ for other strains), which provides $g_d/g_b = A_{zx}/(\sqrt{2}A_v)$.³²⁾ Although such an ideal measurement may be difficult for $A_u = 0$, there are various methods of evaluating different coupling parameters (linear combinations of g_i), which depend on the strain amplitudes a_{U_1} and a_{U_2} (See Sect. S1.2, Supplemental Material).

For a finite A_u/A_v (> 0), $\bar{P}(\varepsilon_0/\omega = 2)$ shows a minimum at ϕ_0 ($0 < \phi_0/\pi < 1/4$ and $3/4 < \phi_0/\pi < 1$) as plotted in Fig. 3, whereas $\phi_0/\pi = 1/4$ and $3/4$ for $A_u = 0$. In the weak coupling limit, ϕ_0 is specified by Eq. (17). As long as A_u/A_v is fixed at a constant, ϕ_0 is not changed by increasing the three couplings as we can see $\phi_0/\pi = 1/6$ and $5/6$ in Fig. 3. For instance, the ratio g_a/g_c can be evaluated by A_u/A_v when we choose $\varepsilon_1 = \varepsilon_{U_2}/2 = \varepsilon_{XY}$.³²⁾ For a single ε_{U_2} , g_e/g_c ($= -\sqrt{2}A_{zx}/A_v$) is determined from the value of $\bar{P}(\varepsilon_0/\omega = 2)$ at $\phi = 0$ as mentioned above. A similar analysis is also useful for evaluating g_a/g_b , g_d/g_b , and various combinations of the spin-strain coupling parameters if the three strain amplitudes a_λ ($\lambda = 1, U_1, U_2$) can be adjusted. On the experimental side of the NV center, unknown coupling parameters related to A_{zx}/A_v have recently been measured using Rabi spectroscopy.²⁰⁾ As a practical application of our theory, this challenging measurement can also be performed by measuring the ultrasonic absorption rate, which is a widely used experimental method.

In the present two-level system based on the $S = 1$ spin with C_{3v} symmetry, the ground state $|\psi_1\rangle$ is responsible for the magnetic moment $M_\parallel = S_x \cos \phi + S_y \sin \phi$. The time-averaged magnetic moment is obtained as $\bar{M}_\parallel = (1 - \bar{P}_{\psi_1 \rightarrow \psi_2}) \sin 2\chi$, where $|\psi_1\rangle$ is chosen as the initial state. Therefore, \bar{M}_\parallel can be controlled by changing the magnetic field strength h as well as the field direction ϕ . Note that \bar{M}_\parallel shows no ϕ dependence when the lattice vibration is absent,

namely, no time-dependent strain is driven. Using Eq. (6), $\sin 2\chi = 2\hbar/\sqrt{9 + 4\hbar^2}$ is obtained. In particular, we focus on $\phi/\pi = 1/2$ in Fig. 1, where \bar{P} completely vanishes in the entire region of ε_0/ω owing to $A_T = 0$. When ϕ/π is tilted slightly from $1/2$, a finite transverse coupling generates an abrupt increase in \bar{P} at $\varepsilon_0/\omega = 1, 2, 3, \dots$, which leads to a sharp resonance peak. Consequently, \bar{M}_\parallel shows an abrupt decrease in the field direction and shrinks by half in the discrete fields $h/\omega = \sqrt{1 - 3D/\omega}$, $\sqrt{2(2 - 3D/\omega)}$, \dots . This can also be realized by optical control using photon-assisted magnetoacoustic resonance.^{21,33)}

In conclusion, we have demonstrated how the spin-strain coupling parameters for the C_{3v} point group are revealed by the magnetoacoustic resonance, especially in the two-phonon transition processes, considering an application to the spin states of the NV center. This phonon transition strongly depends on the change in the longitudinal and transverse quadrupole-strain couplings between the two levels, which can be controlled by rotating a magnetic field around the threefold axis of a defect. The present results provide useful information for high-frequency ultrasonic measurements of quadrupole degrees of freedom inherent in the NV spin state and promote the development of mechanically or ac strain-controlled spin devices.

Acknowledgment This work was supported by JSPS KAKENHI Grant Number 17K05516.

- 1) A. Lenev and S. C. Rand, Phys. Rev. B **53**, 13441 (1996).
- 2) J. P. Goss, R. Jones, S. J. Breuer, P. R. Briddon, S. Öberg, Phys. Rev. Lett. **77**, 3041 (1996).
- 3) A. Gali, M. Fyta, E. Kaxiras, Phys. Rev. B **77**, 155206 (2008).
- 4) M. W. Doherty, N. B. Manson, P. Delaney, and L. C. L. Hollenberg, New J. Phys. **13**, 025019 (2011).
- 5) G. Balasubramanian, P. Neumann, D. Twitchen, M. Markham, R. Kolesov, N. Mizuochi, J. Isoya, J. Achard, J. Beck, J. Tissler, V. Jacques, P. R. Hemmer, F. Jelezko, and J. Wrachtrup, Nat. Mater. **8**, 383 (2009).
- 6) N. Mizuochi, P. Neumann, F. Rempp, J. Beck, V. Jacques, P. Siyushev, K. Nakamura, D. J. Twitchen, H. Watanabe, S. Yamasaki, F. Jelezko, and J. Wrachtrup, Phys. Rev. B **80**, 041201(R) (2009).
- 7) E. D. Herbschleb, H. Kato, Y. Maruyama, T. Danjo, T. Makino, S. Yamasaki, I. Ohki, K. Hayashi, H. Morishita, M. Fujiwara, and N. Mizuochi, Nat. Commun. **10**, 3766 (2019).
- 8) D. Suter and F. Jelezko, Prog. Nucl. Magn. Resonance Spectrosc. **98-99**, 50 (2017).
- 9) P. Udvarhelyi, V. O. Shkolnikov, A. Gali, G. Burkard, and A. Pályi, Phys. Rev. B **98**, 075201 (2018).
- 10) A. Kiel and W. B. Mims, Phys. Rev. B **5**, 803 (1972).
- 11) W. B. Mims, *The Linear Electric Field Effect in Paramagnetic Resonance* (Oxford University Press, Oxford, U. K., 1976).
- 12) E. Van Oort and M. Glasbeek, Chem. Phys. Lett. **168**, 529 (1990).
- 13) M. W. Doherty, F. Dolde, H. Fedder, F. Jelezko, J. Wrachtrup, N. B. Manson, and L. C. L. Hollenberg, Phys. Rev. B **85**, 205203 (2012).
- 14) M. W. Doherty, N. B. Manson, P. Delaney, F. Jelezko, J. Wrachtrup, and L. C. L. Hollenberg, Phys. Rep. **528**, 1 (2013).
- 15) E. R. MacQuarrie, T. A. Gosavi, N. R. Jungwirth, S. A. Bhavé, and G. D. Fuchs, Phys. Rev. Lett. **111**, 227602 (2013).
- 16) P. V. Klimov, A. L. Falk, B. B. Buckley, and D. D. Awschalom, Phys. Rev. Lett. **112**, 087601 (2014).
- 17) A. Barfuss, J. Teissier, E. Neu, A. Nunnenkamp, and P. Maletinsky, Nat. Phys. **11**, 820 (2015).
- 18) D. Lee, K. W. Lee, J. V. Cady, P. Ovartchaiyapong, and A. C. B. Jayich, J. Opt. **19**, 033001 (2017).
- 19) A. Barfuss, M. Kasperczyk, J. Kölbl, and P. Maletinsky, Phys. Rev. B **99**, 174102 (2019).
- 20) H. Y. Chen, S. A. Bhavé, and G. D. Fuchs, Phys. Rev. Appl. **13**, 054068 (2020).

- 21) M. Koga and M. Matsumoto, J. Phys. Soc. Jpn. **89**, 024701 (2020).
- 22) M. Matsumoto and M. Koga, J. Phys. Soc. Jpn. **89**, 084702 (2020).
- 23) T. Goto, H. Yamada-Kaneta, Y. Saito, Y. Nemoto, K. Sato, K. Kakimoto, and S. Nakamura, J. Phys. Soc. Jpn. **75**, 044602 (2006).
- 24) K. Mitsumoto, M. Akatsu, S. Baba, R. Takasu, Y. Nemoto, T. Goto, H. Yamada-Kaneta, Y. Furumura, H. Saito, K. Kashima, and Y. Saito, J. Phys. Soc. Jpn. **83**, 034702 (2014).
- 25) H. Y. Chen, E. R. MacQuarrie, and G. D. Fuchs, Phys. Rev. Lett. **120**, 167401 (2018).
- 26) (Supplemental Material) Information on the complete form of the spin-strain interaction Hamiltonian for the C_{3v} point group is provided online (see Sect. S1.1).
- 27) J. H. Shirley, Phys. Rev. **138**, B979 (1965).
- 28) S.-I. Chu and D. A. Telnov, Phys. Rep. **390**, 1 (2004).
- 29) S.-K. Son, S. Han, and S.-I. Chu, Phys. Rev. A **79**, 032301 (2009).
- 30) J. Hausinger and M. Grifoni, Phys. Rev. A **81**, 022117 (2010).
- 31) I. Gromov and A. Schweiger, J. Magn. Reson. **146**, 110 (2000).
- 32) (Supplemental Material) Discussion on the evaluation of the spin-strain coupling parameters g_i is provided online (see Sect. S1.2).
- 33) (Supplemental Material) Discussion on the time-averaged magnetic moment is provided online, which is associated with a photon-assisted magnetoacoustic resonance (see Sect. S2).

Supplemental Material for 'Magnetoacoustic Resonance to Probe Quadrupole–Strain Coupling in a Diamond Nitrogen-Vacancy Center as a Spin-Triplet System'

Mikito Koga¹ and Masashige Matsumoto²

¹*Department of Physics, Faculty of Education, Shizuoka University, Shizuoka 422–8529, Japan*

²*Department of Physics, Faculty of Science, Shizuoka University, Shizuoka 422–8529, Japan*

S1. Spin–Strain Interaction for $S = 1$ with C_{3v} Symmetry

S1.1 Spin–strain interaction Hamiltonian

We start from the spin–strain interaction Hamiltonian for the spin-1 state with C_{3v} symmetry and next derive a simplified Hamiltonian introducing some constraints to strain tensors. Using the operators for the five quadrupole components expressed by the spin operator $\mathbf{S} = (S_x, S_y, S_z)$ for $S = 1$,

$$\begin{aligned} O_u &= \frac{1}{\sqrt{3}}(2S_z^2 - S_x^2 - S_y^2) = \frac{1}{\sqrt{3}}[3S_z^2 - S(S+1)], \\ O_v &= S_x^2 - S_y^2, \quad O_{xy} = S_x S_y + S_y S_x, \\ O_{zx} &= S_z S_x + S_x S_z, \quad O_{yz} = S_y S_z + S_z S_y, \end{aligned} \quad (\text{S1})$$

the spin–strain interaction Hamiltonian is written as

$$H_\varepsilon = \sum_k A_{k,\varepsilon} O_k \quad (k = u, v, xy, zx, yz), \quad (\text{S2})$$

where $A_{k,\varepsilon}$ is a strain-dependent coupling with each quadrupole O_k . For C_{3v} symmetry, the complete forms of $A_{k,\varepsilon}$ are given as¹⁾

$$\begin{aligned} A_{u,\varepsilon} &= \frac{1}{\sqrt{3}}[h_{41}(\varepsilon_{xx} + \varepsilon_{yy}) + h_{43}\varepsilon_{zz}], \\ A_{v,\varepsilon} &= -\frac{1}{2}\left[h_{16}\varepsilon_{zx} - \frac{1}{2}h_{15}(\varepsilon_{xx} - \varepsilon_{yy})\right], \\ A_{xy,\varepsilon} &= \frac{1}{2}(h_{16}\varepsilon_{yz} + h_{15}\varepsilon_{xy}), \end{aligned}$$

$$\begin{aligned}
A_{zx,\varepsilon} &= \frac{1}{2} \left[h_{26}\varepsilon_{zx} - \frac{1}{2}h_{25}(\varepsilon_{xx} - \varepsilon_{yy}) \right], \\
A_{yz,\varepsilon} &= \frac{1}{2}(h_{26}\varepsilon_{yz} + h_{25}\varepsilon_{xy}).
\end{aligned} \tag{S3}$$

Here, the three basis vectors in the C_{3v} frame are chosen as $\mathbf{e}_x = (-1, -1, 2)/\sqrt{6}$, $\mathbf{e}_y = (1, -1, 0)/\sqrt{2}$, and $\mathbf{e}_z = (1, 1, 1)/\sqrt{3}$. Note that this choice of the x - and y -coordinates is different from the conventional manner. For the latter, the x - and y -axes are parallel to the binary ($[1\bar{1}0]$) and bisectrix ($[11\bar{2}]$) axes, respectively.

$$\varepsilon_{ij} = \frac{1}{2} \left(\frac{\partial u_i}{\partial x_j} + \frac{\partial u_j}{\partial x_i} \right) \tag{S4}$$

denotes the strain tensor with the displacement vector $\mathbf{u} = (u_x, u_y, u_z)$ and $(x_1, x_2, x_3) = (x, y, z)$. The $A_{u,\varepsilon}O_u$ term is equivalent to $\sqrt{3}A_{u,\varepsilon}S_z^2$ except for a common energy shift of the spin states. The spin–strain couplings are characterized by the six independent real parameters h_{41} , h_{43} , h_{15} , h_{16} , h_{25} , and h_{26} .¹⁾ A derivation of H_ε will be shown in Sect. S3.

Next, we transform the strain components in the C_{3v} (xyz) coordinate to those of the cubic crystal (XYZ) coordinate. For the latter, $X \parallel [100]$, $Y \parallel [010]$, and $Z \parallel [001]$. The relationship between the two coordinates is as follows:

$$\begin{aligned}
\varepsilon_{xx} + \varepsilon_{yy} + \varepsilon_{zz} &= \varepsilon_{XX} + \varepsilon_{YY} + \varepsilon_{ZZ} \equiv \varepsilon_B, \\
2\varepsilon_{zz} - \varepsilon_{xx} - \varepsilon_{yy} &= 2(\varepsilon_{YZ} + \varepsilon_{ZX} + \varepsilon_{XY}), \\
\varepsilon_{xx} - \varepsilon_{yy} &= \frac{1}{3}(2\varepsilon_{ZZ} - \varepsilon_{XX} - \varepsilon_{YY}) + \frac{2}{3}(2\varepsilon_{XY} - \varepsilon_{YZ} - \varepsilon_{ZX}), \\
\varepsilon_{zx} &= \frac{1}{3\sqrt{2}}(2\varepsilon_{ZZ} - \varepsilon_{XX} - \varepsilon_{YY}) - \frac{1}{3\sqrt{2}}(2\varepsilon_{XY} - \varepsilon_{YZ} - \varepsilon_{ZX}), \\
\varepsilon_{xy} &= -\frac{1}{2\sqrt{3}}(\varepsilon_{XX} - \varepsilon_{YY}) - \frac{1}{\sqrt{3}}(\varepsilon_{YZ} - \varepsilon_{ZX}), \\
\varepsilon_{yz} &= \frac{1}{\sqrt{6}}(\varepsilon_{XX} - \varepsilon_{YY}) - \frac{1}{\sqrt{6}}(\varepsilon_{YZ} - \varepsilon_{ZX}).
\end{aligned} \tag{S5}$$

To derive these equations, we have used the following transformation

$$\begin{pmatrix} x \\ y \\ z \end{pmatrix} = \begin{pmatrix} -1/\sqrt{6} & -1/\sqrt{6} & 2/\sqrt{6} \\ 1/\sqrt{2} & -1/\sqrt{2} & 0 \\ 1/\sqrt{3} & 1/\sqrt{3} & 1/\sqrt{3} \end{pmatrix} \begin{pmatrix} X \\ Y \\ Z \end{pmatrix}, \tag{S6}$$

and the displacement vector \mathbf{u} follows the same transformation. To simplify the spin–strain interaction Hamiltonian in Eq. (S2), we introduce the following constraints to the strain tensors in the cubic crystal coordinate: $\varepsilon_{XX} = \varepsilon_{YY}$ and $\varepsilon_{YZ} = \varepsilon_{ZX}$. This indicates that the lattice deformations are limited in the plane including both $[001]$ and $[110]$ axes. Consequently, the

above strain-dependent couplings in Eq. (S3) are rewritten as

$$\begin{aligned} A_{u,\varepsilon} &= g_a \varepsilon_1 + g_b \varepsilon_B, \quad A_{v,\varepsilon} = \frac{1}{\sqrt{3}}(g_b \varepsilon_{U_1} + g_c \varepsilon_{U_2}), \\ A_{zx,\varepsilon} &= \frac{1}{\sqrt{6}}(2g_d \varepsilon_{U_1} - g_e \varepsilon_{U_2}), \quad A_{xy,\varepsilon} = A_{yz,\varepsilon} = 0, \end{aligned} \quad (\text{S7})$$

with the bulk strain ε_B and other strain components

$$\begin{aligned} \varepsilon_1 &= \frac{1}{\sqrt{3}}(\varepsilon_{YZ} + \varepsilon_{ZX} + \varepsilon_{XY}), \\ \varepsilon_{U_1} &= \frac{1}{\sqrt{3}}(2\varepsilon_{ZZ} - \varepsilon_{XX} - \varepsilon_{YY}), \\ \varepsilon_{U_2} &= \frac{1}{\sqrt{3}}(2\varepsilon_{XY} - \varepsilon_{YZ} - \varepsilon_{ZX}). \end{aligned} \quad (\text{S8})$$

We disregard ε_B in $A_{u,\varepsilon}$ and consider the simplified spin–strain interaction Hamiltonian [Eq. (1) in the main text] with the five independent coupling constants redefined as

$$\begin{aligned} g_a &= \frac{2}{3}(-h_{41} + h_{43}), \quad g_b = \frac{1}{4}(h_{15} - \sqrt{2}h_{16}), \quad g_c = \frac{1}{4}(2h_{15} + \sqrt{2}h_{16}), \\ g_d &= -\frac{1}{4\sqrt{2}}(h_{25} - \sqrt{2}h_{26}), \quad g_e = \frac{1}{2\sqrt{2}}(2h_{25} + \sqrt{2}h_{26}). \end{aligned} \quad (\text{S9})$$

S1.2 Evaluation of spin–strain coupling parameters g_i ($i = a, b, c, d, e$)

The NV center is a good candidate for investigating the spin–strain couplings in Eq. (S3) and the coupling parameters in Eq. (S9) for the $S = 1$ states with C_{3v} symmetry. The ratio A_{zx}/A_v is related to the spin–strain coupling parameters as

$$\frac{A_{zx}}{A_v} = \frac{2g_d a_{U_1} - g_e a_{U_2}}{\sqrt{2}(g_b a_{U_1} + g_c a_{U_2})} = \frac{-h_{25}(a_{U_1} + 2a_{U_2}) + \sqrt{2}h_{26}(a_{U_1} - a_{U_2})}{h_{15}(a_{U_1} + 2a_{U_2}) - \sqrt{2}h_{16}(a_{U_1} - a_{U_2})}, \quad (\text{S10})$$

where a_λ ($\lambda = 1, U_1, U_2$) represents the amplitude of a time-dependent oscillating strain field ε_λ . Note that ε_λ is defined as Eq. (S8), which is one of the linear combinations of the cubic-frame components of strain tensor. As discussed in the main text, the ratio A_{zx}/A_v is measurable with the two-phonon transition probability. When we choose a single strain component, for instance, ε_{U_1} , the ratio g_d/g_b is given as $g_d/g_b = A_{zx}/(\sqrt{2}A_v)$. Similarly, g_e/g_c can be evaluated by choosing ε_{U_2} . In the presence of two strain components with the amplitudes, for instance, $a_{U_1} = a_{U_2}$, we obtain the information on the coupling parameters in Eq. (S3) as $h_{25}/h_{15} = -A_{zx}/A_v$ [see Eq. (S10)].

In the same manner, the ratio A_u/A_v is given as

$$\frac{A_u}{A_v} = \frac{\sqrt{3}g_a a_1}{g_b a_{U_1} + g_c a_{U_2}} = \frac{8}{\sqrt{3}} \frac{(-h_{41} + h_{43})a_1}{h_{15}(a_{U_1} + 2a_{U_2}) - \sqrt{2}h_{16}(a_{U_1} - a_{U_2})}. \quad (\text{S11})$$

When we choose a single strain component ε_{XY} ($a_1 = a_{U_2}/2$ and $a_{U_1} = 0$) [see Eq. (S8)],

we obtain $g_a/g_c = 2A_u/(\sqrt{3}A_v)$. If the bulk strain ε_B with the amplitude a_B is taken into account as well as the strain ε_1 in Eq. (S11), $g_a a_1$ is just replaced by $g_a a_1 + g_B a_B$, where $g_B = (2h_{41} + h_{43})/(3\sqrt{3})$.

S2. Time-Averaged Magnetic Moment Coupled to Oscillating Strain Fields

In the two-level system based on the $S = 1$ spin with C_{3v} symmetry, the magnetic moment is induced by the singlet ground state $|\psi_1\rangle$ in an applied magnetic field ($\mathbf{h} = \gamma_e \mathbf{H}$), whereas there is no contribution from the excited state $|\psi_2\rangle$. The wave functions $|\psi_1\rangle$ and $|\psi_2\rangle$ are given as Eqs. (4) and (5) in the main text, respectively. Under a magnetic field $(h_x, h_y, h_z) = (h \cos \phi, h \sin \phi, 0)$ perpendicular to $z \parallel [111]$, the matrix form of the spin operator parallel to the field is expressed as

$$M_{\parallel} = S_x \cos \phi + S_y \sin \phi = \begin{pmatrix} \sin 2\chi & 0 \\ 0 & 0 \end{pmatrix}, \quad (\text{S12})$$

using the basis of $\{|\psi_1\rangle, |\psi_2\rangle\}$. When the ground state is chosen as the initial state and the two states are coupled to oscillating strain fields, the time-averaged magnetic moment is obtained as $\bar{M}_{\parallel} = (1 - \bar{P}_{\psi_1 \rightarrow \psi_2}) \sin 2\chi$, where $\bar{P}_{\psi_1 \rightarrow \psi_2}$ is the transition probability and $\sin 2\chi = 2\bar{h}/\sqrt{9 + 4\bar{h}^2}$ is a function of the magnetic field $\bar{h} = h/D$ normalized by the uniaxial crystal field ($3D$ is the level splitting for $h = 0$). At the specific field direction $\phi = \pi/2$ ($[1\bar{1}0]$), the transition probability \bar{P} completely vanishes owing to $A_T = 0$ (see the contour maps in Fig. 1 of the main text). When ϕ is tilted slightly from $\pi/2$, a finite transverse coupling generates an abrupt increase in \bar{P} at $\varepsilon_0/\omega = 1, 2, 3, \dots$, and it causes a sharp resonance peak. Consequently, \bar{M}_{\parallel} shows an abrupt decrease and shrinks by half.

This magnetoacoustic resonance is dominated by the longitudinal coupling with A_L . When the field direction is fixed at $\phi = \pi/2$, the similar resonance can be realized by a hybrid measurement using weak microwave, which has been proposed as photon-assisted magnetoacoustic resonance in our recent study.²⁾ Let us consider the two-level system coupled to a low-frequency photon field oscillating along the z axis ($[111]$), and put an additional photon-mediated coupling strength Δ into the original spin-strain interaction Hamiltonian [Eq. (7) in the main text] as

$$H_{\text{eff}}(t) = \frac{1}{2} \begin{pmatrix} -\tilde{\varepsilon}_0 - A_L \cos \omega t & \Delta \sin \chi + A_T \cos \omega t \\ \Delta \sin \chi + A_T^* \cos \omega t & \tilde{\varepsilon}_0 + A_L \cos \omega t \end{pmatrix}. \quad (\text{S13})$$

Here, $\tilde{\varepsilon}_0 = \omega_0 - \omega_l$ ($\omega_0 \equiv \varepsilon_0/\hbar$) represents the detuning, where ω_l is the photon frequency. This is derived under the rotating wave approximation with respect to ω_l , assuming $\omega_l \ll \omega$. In addition, Δ can be considered as a real number for a sufficiently small photon coupling

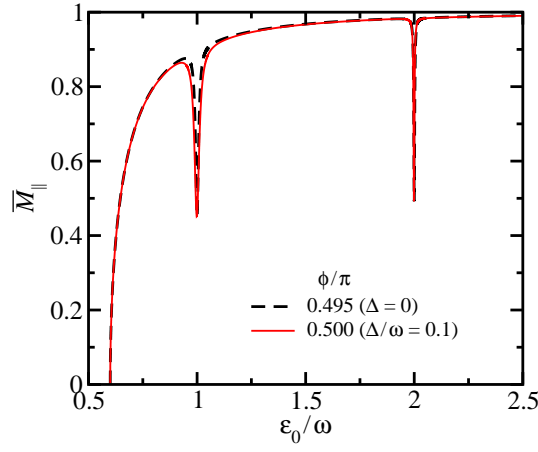


Fig. S1. (Color online) Time-averaged magnetic moment \bar{M}_{\parallel} induced by a magnetic field in the direction of $(\cos \phi, \sin \phi, 0)$ (the z axis is chosen as the threefold axis), which is plotted as a function of ε_0/ω for $D = 0.2$ and $(A_u, A_v, A_{zx}) = (0, 0.4, 0.4)$ in units of ω . This is a comparison of the data (black dashed line) for $\phi/\pi = 0.495$ and $\Delta = 0$ (no photon field) with the data (red solid line) for $\phi/\pi = 0.5$ and $\Delta/\omega = 0.1$ (weak photon field). The energy splitting ε_0 between the two states is related to the magnetic field h as $\varepsilon_0/D = [3 + \sqrt{9 + 4(h/D)^2}]/2$.

compared to the quadrupole–strain coupling with A_L or A_T .²⁾ Since Δ in the off-diagonal component in Eq. (S13) represents the photonic transition, the Δ term causes the transition between the two states even for $A_T = 0$.

In Fig. S1, we compare the results of \bar{M}_{\parallel} as a function of ε_0/ω ($\varepsilon_0 > 3D$): One is the result for the transverse-phonon coupling effect ($|A_T| \ll |A_L|$, $\Delta = 0$) at $\phi/\pi = 0.495$ and the other is that for the photon-assisted longitudinal-phonon coupling effect ($|\Delta| \ll |A_L|$, $A_T = 0$) at $\phi/\pi = 0.5$. It is evident that both results are almost identical, which indicates the equivalency of the phonon- and photon-mediated transverse couplings in the transition between the two levels. Note that the former coupling is induced by an oscillating strain field driven by an acoustic wave or a mechanical oscillator, whereas the latter is due to an ac magnetic field of a microwave with a background of a high-frequency strain field. In Fig. S1, the abrupt shrinking of \bar{M}_{\parallel} occurs at $\varepsilon_0/\omega = 1, 2, 3, \dots$, and the dips in the \bar{M}_{\parallel} curve become narrower as ε_0 increases. As mentioned above, $\phi = \pi/2$ is a specific field direction ($[1\bar{1}0]$) associated with the abrupt change in \bar{M}_{\parallel} at the discrete values of the magnetic field $h/\omega = \sqrt{1 - 3D/\omega}$, $\sqrt{2(2 - 3D/\omega)}$, \dots , and these values correspond to $\varepsilon_0/\omega = 1, 2, \dots$, respectively. This is a very unique point for the present magnetoacoustic resonance, which also holds for the strong spin–strain coupling.

S3. Derivation of Spin–Strain Interaction Hamiltonian

In this section, we derive the complete form of the spin–strain interaction Hamiltonian in Eqs. (S2) and (S3) for C_{3v} symmetry using a group theoretical analysis.^{3–7)} Let us start from the general expression in the following form:

$$H_{\varepsilon} = \sum_{ijkl} K_{ijkl} S_i S_j \varepsilon_{kl} \quad (i, j, k, l = x, y, z). \quad (\text{S14})$$

Here, the strain tensor ε_{kl} is defined by Eq. (S4), and S_i is the i component of spin operator. The coefficient K_{ijkl} represents the coupling of quadrupoles (products of spin operators) and strains. The strain tensor is symmetric ($\varepsilon_{kl} = \varepsilon_{lk}$) and there are six degrees of freedom for kl in K_{ijkl} . Since H_{ε} is invariant under the time-reversal transformation, K_{ijkl} is real. To satisfy the Hermitian nature of the Hamiltonian, it must be symmetric ($K_{ijkl} = K_{jikl}$). This leads to $K_{ijkl}(S_i S_j + S_j S_i) = K_{ijkl} O_{ij}$ for $i \neq j$, where O_{ij} is given by Eq. (S1). Since O_{ij} is symmetric as ε_{kl} , there are six degrees of freedom for ij in K_{ijkl} . Thus, K_{ijkl} is a real symmetric tensor with respect to both $i \leftrightarrow j$ and $k \leftrightarrow l$, and it can be reduced to a 6×6 matrix.

The spin–strain interaction Hamiltonian is then rewritten as

$$H_{\varepsilon} = \sum_{m,n=x,x,y,y,z,z,yz,zx,xy} \tilde{K}_{mn} \tilde{O}_m \tilde{\varepsilon}_n. \quad (\text{S15})$$

Here, the vectorial components with tilde are defined by the six tensorial components as⁵⁾

$$\begin{aligned} \tilde{O}_m &\longrightarrow \left(O_{xx}, O_{yy}, O_{zz}, \sqrt{2} \frac{O_{yz}}{2}, \sqrt{2} \frac{O_{zx}}{2}, \sqrt{2} \frac{O_{xy}}{2} \right), \\ \tilde{\varepsilon}_n &\longrightarrow (\varepsilon_{xx}, \varepsilon_{yy}, \varepsilon_{zz}, \sqrt{2} \varepsilon_{yz}, \sqrt{2} \varepsilon_{zx}, \sqrt{2} \varepsilon_{xy}), \end{aligned} \quad (\text{S16})$$

where $O_{ii} = S_i^2$. The matrix \tilde{K} in Eq. (S15) is determined so as to satisfy the invariance of H_{ε} under the symmetry transformations. This type of tensor \tilde{K}_{mn} is known as a fourth-rank matter tensor.^{4–6)} For the C_{3v} point group, it is given by⁵⁾

$$\tilde{K}_{mn} \longrightarrow \begin{pmatrix} K_{11} & K_{12} & K_{13} & \frac{K_{14}}{\sqrt{2}} & 0 & 0 \\ K_{12} & K_{11} & K_{13} & -\frac{K_{14}}{\sqrt{2}} & 0 & 0 \\ K_{31} & K_{31} & K_{33} & 0 & 0 & 0 \\ \frac{K_{41}}{\sqrt{2}} & -\frac{K_{41}}{\sqrt{2}} & 0 & \frac{K_{44}}{2} & 0 & 0 \\ 0 & 0 & 0 & 0 & \frac{K_{44}}{2} & K_{41} \\ 0 & 0 & 0 & 0 & K_{14} & K_{11} - K_{12} \end{pmatrix}, \quad (\text{S17})$$

using the basis of the vectors in Eq. (S16). Substituting Eqs. (S16) and (S17) for Eq. (S15),

we obtain

$$\begin{aligned}
H_\varepsilon = & K_{11}(\varepsilon_{xx}O_{xx} + \varepsilon_{yy}O_{yy}) + K_{33}\varepsilon_{zz}O_{zz} + K_{12}(\varepsilon_{yy}O_{xx} + \varepsilon_{xx}O_{yy}) \\
& + K_{13}\varepsilon_{zz}(O_{xx} + O_{yy}) + K_{31}(\varepsilon_{xx} + \varepsilon_{yy})O_{zz} + \frac{K_{44}}{2}(\varepsilon_{yz}O_{yz} + \varepsilon_{zx}O_{zx}) + (K_{11} - K_{12})\varepsilon_{xy}O_{xy} \\
& + K_{14}\varepsilon_{yz}O_v + \frac{K_{41}}{2}\varepsilon_vO_{yz} + K_{14}\varepsilon_{zx}O_{xy} + K_{41}\varepsilon_{xy}O_{zx},
\end{aligned} \tag{S18}$$

where $\varepsilon_v = \varepsilon_{xx} - \varepsilon_{yy}$. Using $O_{xx} + O_{yy} + O_{zz} = S(S + 1)$ for spin S , this is rewritten as

$$\begin{aligned}
H_\varepsilon = & \frac{1}{2}(2K_{31} - K_{11} - K_{12})(\varepsilon_{xx} + \varepsilon_{yy})O_{zz} + (K_{33} - K_{13})\varepsilon_{zz}O_{zz} \\
& + \frac{1}{2}[(K_{11} - K_{12})\varepsilon_v + 2K_{14}\varepsilon_{yz}]O_v + [(K_{11} - K_{12})\varepsilon_{xy} + K_{14}\varepsilon_{zx}]O_{xy} \\
& + \frac{1}{2}(K_{44}\varepsilon_{yz} + K_{41}\varepsilon_v)O_{yz} + \frac{1}{2}(K_{44}\varepsilon_{zx} + 2K_{41}\varepsilon_{xy})O_{zx}.
\end{aligned} \tag{S19}$$

Here, the terms of a common energy shift have been neglected. Note that the axis vectors of the xyz coordinate are defined as $\mathbf{e}_x = (1, -1, 0)/\sqrt{2}$, $\mathbf{e}_y = (1, 1, -2)/\sqrt{6}$, and $\mathbf{e}_z = (1, 1, 1)/\sqrt{3}$.

Following Udvarhelyi et al.,¹⁾ we finally convert the axis vectors as $\mathbf{e}_x \rightarrow \mathbf{e}_y$ and $\mathbf{e}_y \rightarrow -\mathbf{e}_x$ to compare H_ε derived here with the Hamiltonian in Eqs. (S2) and (S3). The latter was previously derived in Ref. 1. Accordingly, the subscripts and signs of the strain tensors and quadrupole operators are replaced as $yz \rightarrow -zx$, $zx \rightarrow yz$, $xy \rightarrow -xy$, and $v \rightarrow -v$. For the spin-strain coupling coefficients, $K_{14} \rightarrow K_{15}$ and $K_{41} \rightarrow K_{51}$. The obtained Hamiltonian is then rewritten as

$$\begin{aligned}
H_\varepsilon = & \frac{1}{2}(2K_{31} - K_{11} - K_{12})(\varepsilon_{xx} + \varepsilon_{yy})O_{zz} + (K_{33} - K_{13})\varepsilon_{zz}O_{zz} \\
& + \frac{1}{2}[(K_{11} - K_{12})\varepsilon_v + 2K_{15}\varepsilon_{zx}]O_v + [(K_{11} - K_{12})\varepsilon_{xy} - K_{15}\varepsilon_{yz}]O_{xy} \\
& + \frac{1}{2}(K_{44}\varepsilon_{zx} + K_{51}\varepsilon_v)O_{zx} + \frac{1}{2}(K_{44}\varepsilon_{yz} - 2K_{51}\varepsilon_{xy})O_{yz}.
\end{aligned} \tag{S20}$$

As a result, the spin-strain coupling parameters in Eq. (S2) are related to those in Eq. (S20) as follows:

$$\begin{aligned}
h_{41} = & \frac{1}{2}(2K_{31} - K_{11} - K_{12}), \quad h_{43} = K_{33} - K_{13}, \\
h_{15} = & 2(K_{11} - K_{12}), \quad h_{16} = -2K_{15}, \\
h_{25} = & -2K_{51}, \quad h_{26} = K_{44}.
\end{aligned} \tag{S21}$$

References

- 1) P. Udvarhelyi, V. O. Shkolnikov, A. Gali, G. Burkard, and A. Pályi, Phys. Rev. B **98**, 075201 (2018).
- 2) M. Koga and M. Matsumoto, J. Phys. Soc. Jpn. **89**, 024701 (2020).
- 3) P. L. Donoho, Phys. Rev. **133**, A1080 (1964).
- 4) J. F. Nye, *Physical Properties of Crystals: Their Representation by Tensors and Matrices* (Oxford University Press, New York, 1985).
- 5) A. S. Nowick, *Crystal Properties via Group Theory* (Cambridge University Press, New York, 1995).
- 6) R. C. Powell, *Symmetry, Group Theory, and the Physical Properties of Crystals* (Springer, New York, 2010).
- 7) M. Matsumoto and M. Koga, J. Phys. Soc. Jpn. **89**, 084702 (2020).